Journal of Computational Physics **179,** 439–451 (2002)
doi:10.1006/jcph.2002.7064

Comparison of the Lattice Boltzmann Method and the Artificial Compressibility Method for Navier–Stokes Equations

Xiaoyi He, Gary D. Doolen, and T. Clark

Theoretical Division, Los Alamos National Laboratory, Los Alamos, New Mexico 87545
E-mail: hex@apci.com

Received July 18, 2001; revised March 5, 2002

This paper compares in detail the lattice Boltzmann method and an isothermal Navier–Stokes method. It is found that these two methods are closely related to each other. Both methods satisfy similar macroscopic governing equations in their continuous forms, but they differ from each other in their discrete forms. Besides the obvious differences in stencils for spatial discretization, these two methods also differ from each other in temporal discretization. Numerical tests show that these differences have little impact on the simulation of velocity fields but do generate noticeable differences in the pressure fields. Both methods are capable of simulating transient flows and exhibit oscillatory behavior due to the propagation of pressure waves. The lattice Boltzmann method may be more accurate for capturing the pressure waves.

I. INTRODUCTION

The lattice Boltzmann method (LBM) as a new computational fluid dynamics (CFD) tool has received considerable attention in recent years (see, e.g., [1]). This method can be regarded as either an extension of the lattice gas automaton [2, 3] or a special discrete form of the Boltzmann equation from kinetic theory [4]. Although the connection between the gas kinetic theory and hydrodynamics has long been established [5], the lattice Boltzmann method needs additional special discretization of velocity space to recover the correct hydrodynamics. Due to the very same reason, the LBM works exactly opposite traditional CFD methods in deriving working schemes: LBM uses Navier–Stokes equations as its target while traditional CFD methods use Navier–Stokes equations as their starting point. Not surprisingly, the exact relation between the LBM and traditional CFD schemes based on directly solving Navier–Stokes equations has not been well understood.

0021-9991/02 $35.00

This lack of a clear relation between the LBM and other CFD methods makes it difficult to assess the relative strengths of LBM and traditional CFD methods. In fact, most of the existing knowledge of the LBM's performance has been accumulated through numerical LBM experiments (e.g., [6–8]). Although these benchmark studies demonstrated the LBM's accuracy in simulating fluid flows, few comparisons were made of the relative computational efficiency of the LBM and other CFD methods. Part of the reason for this is that it is unclear with which classical method LBM should be compared. Most of the conventional CFD methods have been developed either for incompressible flow or for strongly compressible flow. The LBM is applicable to the isothermal flow regime, i.e., the weakly compressible, low-Mach-number limit. This flow regime is traditionally treated as "incompressible," although there are CFD methods constructed to compute the Navier–Stokes equations in this regime. The argument for treating very low-Mach-number flows as incompressible is pragmatic rather than physical—the direct calculation of the isothermal Navier–Stokes equations requires time steps sufficiently small to resolve acoustic waves across a computational cell. This time step may be vastly smaller than the time scales of interest for the bulk fluid motion. Thus the computational cost of the many additional time steps required by an isothermal calculation may be vastly higher than the cost of an incompressible calculation. Of course, in reality there is no fluid or flow that is absolutely incompressible (i.e., with infinite acoustic velocity).

The artificial compressibility (AC) method was introduced by Chorin [9] 30 years ago. The basic idea was to substitute an artificially low sound speed and to compute the resulting isothermal equations using as large a time step as permissible from the standpoint of numerical stability. The intent was not to produce time-accurate results but to accelerate the convergence to a time-steady, nearly incompressible field. For the circumstance of an LBM wherein the acoustic velocity is not scaled to that of an actual fluid being simulated, the LBM method also resembles an AC method.

The goal of this study is to begin to bridge the gap between the isothermal equations, artificial compressibility methods, LBM and incompressible Navier–Stokes methods. To be specific, we demonstrate that the lattice Boltzmann method is closely related to the numerical methods for solving the isothermal equations, and hence also to the artificial compressibility (AC) method proposed by Chorin. This connection has been conjectured before. He and Luo [10] demonstrated that in the limit of incompressible flow for which LBM is most suitable, the lattice Boltzmann equation recovers governing equations similar to the isothermal Navier–Stokes equations that the artificial compressibility method was based on. What has been missing in the literature is a direct comparison of the discrete forms and a careful numerical comparison of these methods. As revealed by this study, the LBM indeed differs in its discrete form from the finite-difference representations of the isothermal Navier–Stokes equations as given by the artificial compressibility method. However, as our numerical tests show, these differences have little impact on the simulated velocity fields, although they do generate noticeably different pressure fields.

To simplify our analysis, this study only focuses on single-phase flow. We notice that, as a simulation tool based on kinetic theory, the lattice Boltzmann method has the potential to incorporate microscopic physics, such as intermolecular interactions. This feature enables use of the LBM to study effectively many complex phenomena, including spinodal decomposition [11], amphiphilic fluid flows [12], and multiphase flows [13]. Although this work does not touch on these topics, it helps to evaluate the accuracy and efficiency of the lattice Boltzmann models for these complex phenomena for future use.

The rest of the paper is organized as follows. Section II describes the lattice Boltzmann method in the weakly compressible limit. Derivations were made to regroup the lattice Boltzmann equation into a form comparable with the artificial compressibility method. Section III presents detailed comparisons between the LBM and the artificial compressibility method. Section IV presents numerical comparisons of these two methods. Section V concludes the paper.

II. LATTICE BOLTZMANN EQUATION

Unlike the Boltzmann equation, the lattice Boltzmann equation works best for isothermal, weakly compressible flow. The reason for this has been discussed extensively in the literature. We refer interested readers to the review by Chen and Doolen [1]. Here we only focus on the lattice Boltzmann method applied to a single-phase, isothermal, weakly compressible flow.

The lattice Boltzmann BGK model for Navier–Stokes equations for weakly compressible flows has the form

$$f_\alpha(\mathbf{x}, t+\delta_t) = f(\mathbf{x} - M^{-1}\mathbf{e}_a\delta_t, t) - \frac{f(\mathbf{x} - M^{-1}\mathbf{e}_a\delta_t, t) - f^{eq}(\mathbf{x} - M^{-1}\mathbf{e}_a\delta_t, t)}{\tau}\delta_t, \quad (1)$$

where f_α is the density distribution function, $\mathbf{e}_a$ is the discrete velocity (lattice velocity), τ is the relaxation time, and δ_t is the simulation time step. The equilibrium distribution f_α^{eq} is given by

$$f_\alpha^{eq} = w_\alpha[pM^2 + \mathbf{e}_a \cdot \mathbf{u}M + 0.5(\mathbf{e}_a \cdot \mathbf{u})^2M^2 - 0.5\mathbf{u}^2M^2], \quad (2)$$

where $M = U/c_s$ is the Mach number, with U being a characteristic macroscopic velocity and c_s being the sound speed; w_α is the integral coefficient. All the variables are dimensionless. The characteristic variables are ρ_0U^2 for pressure (ρ_0 for fluid density), U for macroscopic velocity, L for length, L/U for time, and c_s for lattice velocity. Here we use a scaling of the lattice velocity which differs from those in conventional lattice Boltzmann literature. In the conventional lattice Boltzmann literature, the lattice velocities are usually scaled by the lattice speed $c = \delta_x/\delta_t$.

The pressure and macroscopic velocity are calculated using

$$p = M^{-2}\sum_\alpha f_\alpha, \quad (3)$$

$$\mathbf{u} = M^{-1}\sum_\alpha f_\alpha \mathbf{e}_a. \quad (4)$$

The choice for the underlying lattice velocities and their corresponding integral coefficients is not unique, but they must satisfy [10, 14]

$$\sum_\alpha w_\alpha \mathbf{e}_a^{2n+1} = 0, \quad (5)$$

$$\sum_\alpha w_\alpha \mathbf{e}_a^{2n} = \boldsymbol{\delta}^n, \quad (6)$$

for $n = 0, 1, 2$; $\boldsymbol{\delta}$ is the delta function as defined in [15].

To second order in the Enskog–Chapman expansion, the above lattice Boltzmann BGK model recovers the macroscopic equation [4]

$$M^2\frac{\partial p}{\partial t}+\nabla\cdot\mathbf{u}=0, \tag{7}$$

$$\frac{\partial \mathbf{u}}{\partial t}+\mathbf{u}\cdot\nabla\mathbf{u}=-\nabla p+\frac{1}{Re}\nabla^2\mathbf{u}+\frac{1}{Re}\nabla(\nabla\cdot\mathbf{u}), \tag{8}$$

where $Re=UL/\nu$ is the Reynolds number, with ν the kinematic viscosity. In nondimensional form, the relaxation time is related to the Reynolds number and Mach number via $\tau=M^2/Re+0.5\delta_t$.

The above lattice Boltzmann model has a linear dependence on pressure. This implies that we can replace the real pressure by the pressure perturbation around its average value. With this substitution, we can ensure that the nondimensional pressure term is first order.

Equations (7) and (8) are not the incompressible Navier–Stokes equations except for steady flows. In fact, they bear a striking similarity to the perturbed equations used by Chorin in the artificial compressibility method for the steady Navier–Stokes equations [9]

$$\frac{\partial p}{\partial t}+c^2\nabla\cdot\mathbf{u}=0, \tag{9}$$

$$\frac{\partial \mathbf{u}}{\partial t}+\nabla\cdot(\mathbf{uu})=-\nabla p+\frac{1}{Re}\nabla^2\mathbf{u}. \tag{10}$$

The parameter c in the artificial compressibility method corresponds to $1/M$ in the lattice Boltzmann method. The only difference between these two methods is that the momentum equation of the lattice Boltzmann method has the additional term of $\nabla(\nabla\cdot\mathbf{u})/Re$. This term vanishes when steady states are approached.

To compare further the lattice Boltzmann method with the artificial compressibility method, we transform the above LBM model by expanding the right hand side of Eq. (1) around $(\mathbf{x}, t)$,

$$\begin{aligned} f_\alpha(\mathbf{x},t+\delta_t) &= f_\alpha^{eq}(\mathbf{x}-M^{-1}\mathbf{e}_a\delta_t,t)+\left(1-\frac{\delta_t}{\tau}\right)f_\alpha^1(\mathbf{x}-M^{-1}\mathbf{e}_a\delta_t,t)\\ &= f_\alpha^{eq}-\delta_t M^{-1}(\mathbf{e}_a\cdot\nabla)f_\alpha^{eq}+\frac{\delta_t^2}{2}M^{-2}(\mathbf{e}_a\cdot\nabla)^2 f_\alpha^{eq}+\frac{\delta_t^3}{6}M^{-3}(\mathbf{e}_a\cdot\nabla)^3 f_\alpha^{eq}\\ &\quad+\left(1-\frac{\delta_t}{\tau}\right)\left[f_\alpha^1-\delta_t M^{-1}(\mathbf{e}_a\cdot\nabla)f_\alpha^1+\frac{\delta_t^2M^{-2}}{2}(\mathbf{e}_a\cdot\nabla)^2 f_\alpha^1\right], \end{aligned} \tag{11}$$

where $f_\alpha^1=f_\alpha-f_\alpha^{eq}$. This expansion presumed a condition of $\delta_t/M\ll 1$, which is usually satisfied in most simulations. Summation of Eq. (11) over α yields

$$\begin{aligned} p(\mathbf{x},t+\delta_t)M^2 &= p(\mathbf{x},t)M^2-\delta_t\nabla\cdot\mathbf{u}+\frac{\delta_t^2}{2}[\nabla^2 p+\nabla\cdot\mathbf{A}]-\frac{\delta_t^3M^{-2}}{2}\nabla\nabla:\mathbf{S}\\ &\quad-(\tau-\delta_t)\frac{\delta_t^2M^{-2}}{2}\nabla\nabla:\mathbf{S}, \end{aligned} \tag{12}$$

or

$$p(\mathbf{x},t+\delta_t)=p(\mathbf{x},t)-\delta_t M^{-2}\nabla\cdot\left[\mathbf{u}-\frac{\delta_t}{2}\left(\nabla p+\mathbf{A}-\frac{1}{Re}\nabla\cdot\mathbf{S}\right)\right], \tag{13}$$

where $\mathbf{A} = \nabla \cdot (\mathbf{uu})$ is the convection term and $\mathbf{S} = \nabla \mathbf{u} + (\nabla \mathbf{u})^T$ (see the Appendix for more details of the moment summations of f^{eq} and f^1).

Multiplying Eq. (11) by $\mathbf{e}_a$ and summing over α, we have

$$\mathbf{u}(\mathbf{x}, t + \delta_t)M = \mathbf{u}(\mathbf{x}, t)M - \delta_t M(\nabla p + \mathbf{A}) + \frac{\delta_t^2 M^{-1}}{2}[\nabla^2 \mathbf{u} + 2\nabla(\nabla \cdot \mathbf{u})] + (\tau - \delta_t)\delta_t M^{-1}[\nabla^2 \mathbf{u} + \nabla(\nabla \cdot \mathbf{u})], \tag{14}$$

or

$$\mathbf{u}(\mathbf{x}, t + \delta_t) = \mathbf{u}(\mathbf{x}, t) - \delta_t \left[\nabla \left(p - \frac{\delta_t}{2} M^{-2} \nabla \cdot \mathbf{u} \right) + \mathbf{A} - \frac{1}{Re} \nabla \cdot \mathbf{S} \right]. \tag{15}$$

To order δ_t^2, we have

$$\bar{p} = p(\mathbf{x}, t) - \frac{\delta_t}{2} M^{-2} \nabla \cdot \mathbf{u} + O\left(\delta_t^2\right), \tag{16}$$

$$\bar{\mathbf{u}} = \mathbf{u}(\mathbf{x}, t) - \frac{\delta_t}{2} \left(\nabla p + A - \frac{1}{Re} \nabla \cdot \mathbf{S} \right) + O\left(\delta_t^2\right), \tag{17}$$

where $\bar{p} = [p(\mathbf{x}, t + \delta_t) + p(\mathbf{x}, t)]/2$ and $\bar{\mathbf{u}} = [\mathbf{u}(\mathbf{x}, t + \delta_t) + \mathbf{u}(\mathbf{x}, t)]/2$. With the help of Eqs. (16) and (17), the discrete equations for pressure and velocity finally become

$$p(\mathbf{x}, t + \delta_t) = p(\mathbf{x}, t) - \delta_t M^{-2} \nabla \cdot \bar{\mathbf{u}} + O\left(\delta_t^3\right), \tag{18}$$

$$\mathbf{u}(\mathbf{x}, t + \delta_t) = \mathbf{u}(\mathbf{x}, t) - \delta_t \left[\nabla \bar{p} + \mathbf{A} - \frac{1}{Re} \nabla \cdot \mathbf{S} \right] + O\left(\delta_t^3\right). \tag{19}$$

As shown in the next section, Eqs. (18) and (19) are closely related to the evolution equation of the artificial compressibility method.

III. COMPARISON OF THE LATTICE BOLTZMANN METHOD WITH THE ARTIFICIAL COMPRESSIBILITY METHOD

The artificial compressibility (AC) method was first proposed by Chorin [9] for solving approximating the steady-state incompressible Navier–Stokes equations. This method introduces a perturbed continuity equation, Eq. (9). For incompressible flow, Eq. (9) has no physical meaning except for the steady state. The coefficient c is merely a numerical parameter controlling the convergence rate to steady states. For compressible flow, however, Eq. (9) does have a physical meaning. In fact, it can be derived from the Navier–Stokes equations for compressible fluids with the equation of state, $p = c^2 \rho$, where c is the sound speed. This is why the name "artificial compressibility method" is used in the first place. In this regard, this method is actually not "artificial" if applied to weakly compressible fluids with a constant sound speed. Under this circumstance, it is an isothermal Navier–Stokes method.

There are many ways to discretize the artificial compressibility method. A typical one uses explicit discretization in time and staggered discretization in space. It has been shown that the staggered grid is necessary to prevent unsatisfactory pressure oscillations [17]. A

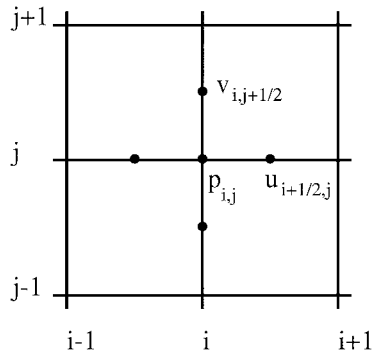

FIG. 1. A typical marker-and-cell (MAC) mesh.

useful staggered grid is the marker-and-cell (MAC) grid introduced by Harlow and Welch [18] (Fig. 1). Note that velocities and pressures are evaluated at different grid points. The discrete equations of the artificial compressibility method on a MAC grid have the form

$$\frac{1}{\delta_t}\left(u^{n+1}_{i+1/2,j} - u^n_{i+1/2,j}\right) + a^n_{i+1/2,j} + \Delta_x p^n_{i+1/2,j} = \frac{1}{Re}\nabla_h^2 u^n_{i+1/2,j}, \tag{20}$$

$$\frac{1}{\delta_t}\left(v^{n+1}_{i,j+1/2} - u^n_{i,j+1/2}\right) + b^n_{i,j+1/2} + \Delta_y p^n_{i,j+1/2} = \frac{1}{Re}\nabla_h^2 v^n_{i,j+1/2}, \tag{21}$$

$$\frac{1}{\delta_t}\left(p^{n+1}_{i,j} - p^n_{i,j}\right) + c^2\left(\Delta_x u^{n+1}_{i,j} + \Delta_y v^{n+1}_{i,j}\right) = 0, \tag{22}$$

where the difference operators Δ_x, Δ_y, and ∇_h^2 are defined by

$$\Delta_x f_{i,j} = \frac{1}{\Delta_x}\left(f_{i+1/2,j} - f_{i-1/2,j}\right), \tag{23}$$

$$\Delta_y f_{i,j} = \frac{1}{\Delta_x}\left(f_{i,j+1/2} - f_{i,j-1/2}\right), \tag{24}$$

$$\nabla_h^2 f_{i,j} = (\Delta_x\Delta_x + \Delta_y\Delta_y) f_{i,j}. \tag{25}$$

The terms $a^n_{i+1/2,j}$ and $b^n_{i,j+1/2}$ are the approximations of the components of vector $\mathbf{A}$. Obviously, the discretization stencils of the artificial compressibility method are quite different from those in the lattice Boltzmann method. However, if we neglect this difference and use the continuous form, Eqs. (20)–(22) can be written as

$$\mathbf{u}^{n+1} = \mathbf{u}^n - \delta_t\left(\nabla p^n + \mathbf{A}^n - \frac{1}{Re}\nabla^2\mathbf{u}^n\right), \tag{26}$$

$$p^{n+1} = p^n - \delta_t c^2 \nabla\cdot\mathbf{u}^{n+1}. \tag{27}$$

Considering the fact that the superscripts $n+1$ and n stand for the new and old time steps and $c = 1/M$, it is easy to make a direct comparison between the discrete equations of the lattice Boltzmann method and the artificial compressibility method. The most important difference is that the values of the velocity and pressure averaged over n and $n+1$ are used in the lattice Boltzmann method in calculating new variables. In the artificial compressibility

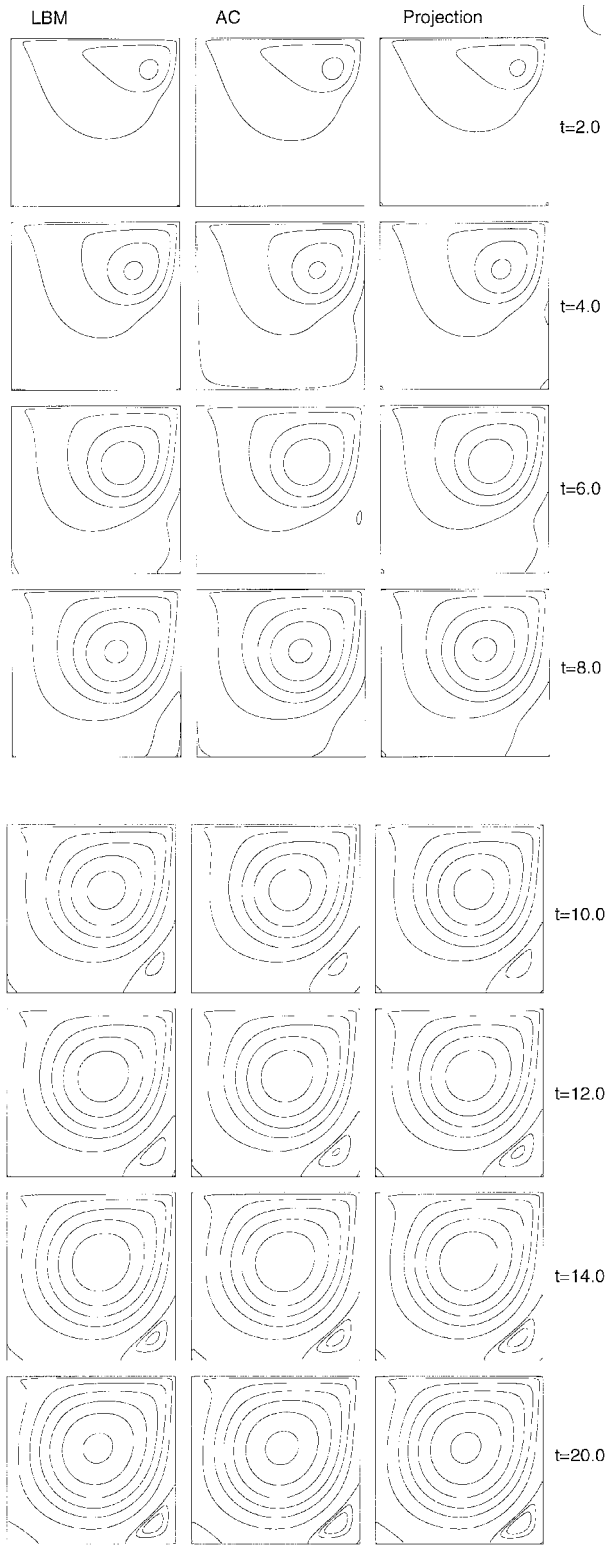

FIG. 2. Comparison of velocity field evolution simulated using the lattice Boltzmann, artificial compressibility, and projection methods. The flow fields are illustrated using iso-streamline contour plots.

method, variables at either the last time step (pressure) or at the present time step (velocity) are used in the evolution. Using the average value helps to reduce errors associated with temporal discretization and that is why the lattice Boltzmann method has second-order accuracy in time.

The above differences in the stencils for spatial discretization and the scheme for temporal discretization are not expected to generate significant differences on the simulation results. We will see this in the next section.

IV. NUMERICAL SIMULATIONS

To confirm our theoretical analysis, we carried out numerical simulations comparing the lattice Boltzmann method and the artificial compressibility method. We use cavity flow as our test case. Simulations start from a quiescent state with uniform pressure inside the

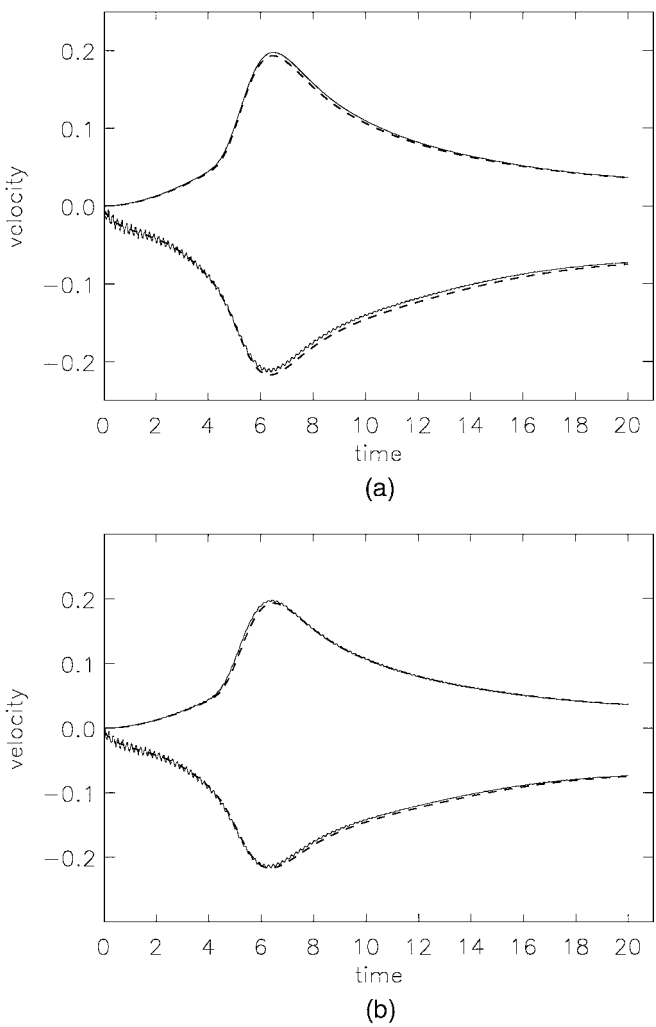

FIG. 3. Time history of velocity at the cavity center. Results from both (a) the lattice Boltzmann and (b) artificial compressibility methods exhibit oscillations. Otherwise they compare well with results from the projection method (dashed lines).

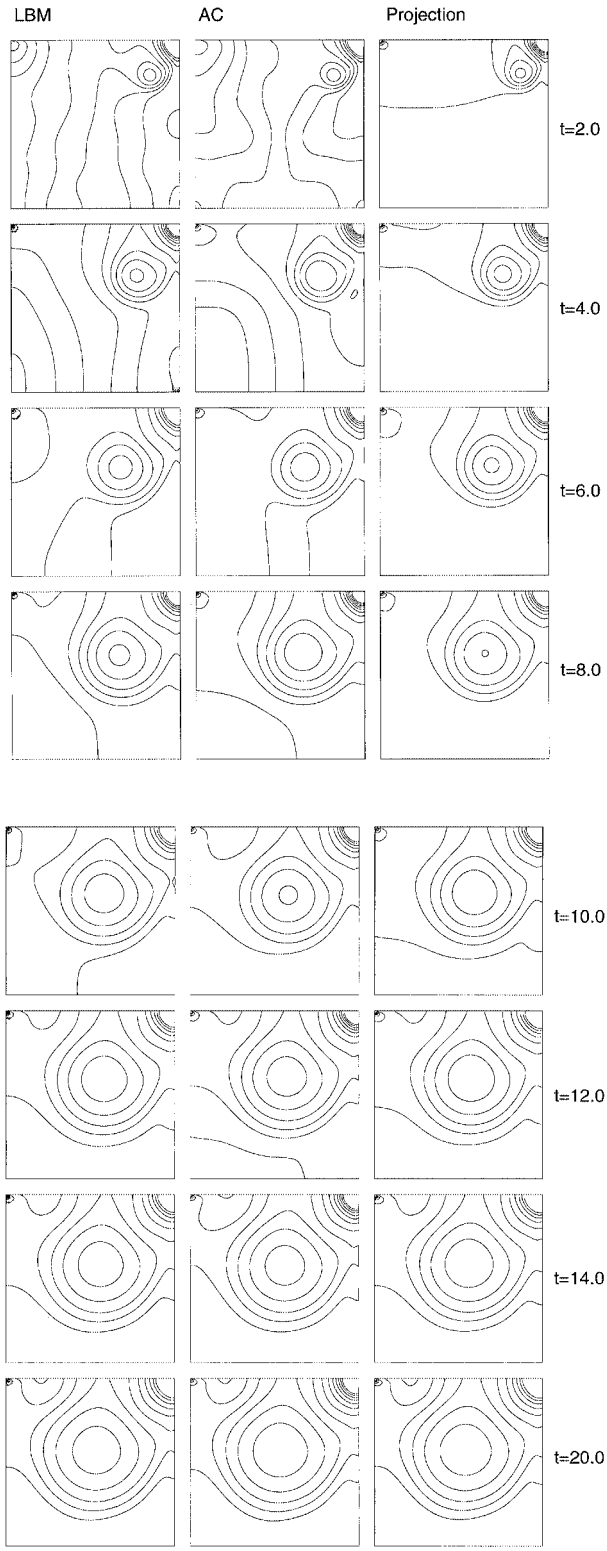

FIG. 4. Comparison of evolution of velocity fields simulated using the lattice Boltzmann, artificial compressibility, and projection methods.

cavity. The top lid starts moving at a constant velocity at $t = 0$. We follow the evolution of the flow field all the way to the final steady state. The simulations were carried out at a Reynolds number of 1000 and a Mach number of 0.087. A 256×256 mesh was used for all simulations. The computational speeds for the two methods are comparable.

Figure 2 shows the time evolution of the iso-streamline contours simulated using the lattice Boltzmann method and the artificial compressibilility method, as well as the projection method. The projection method is very accurate for simulating unsteady incompressible flow [17]. As shown, there is little difference among the simulated flow fields. The steady–steady results also agree with those in published studies (e.g., [7, 19]).

Like the artificial compressibility method, the lattice Boltzmann method generates a small oscillation around the primary results due to its compressible nature. Figure 3 compares the time histories of the velocity at the middle of the cavity by LBM, AC, and projection methods. The oscillation is noticeable in the very beginning and gradually dissipates as time increases. The average period of these small oscillation is about 0.17. This agrees well with

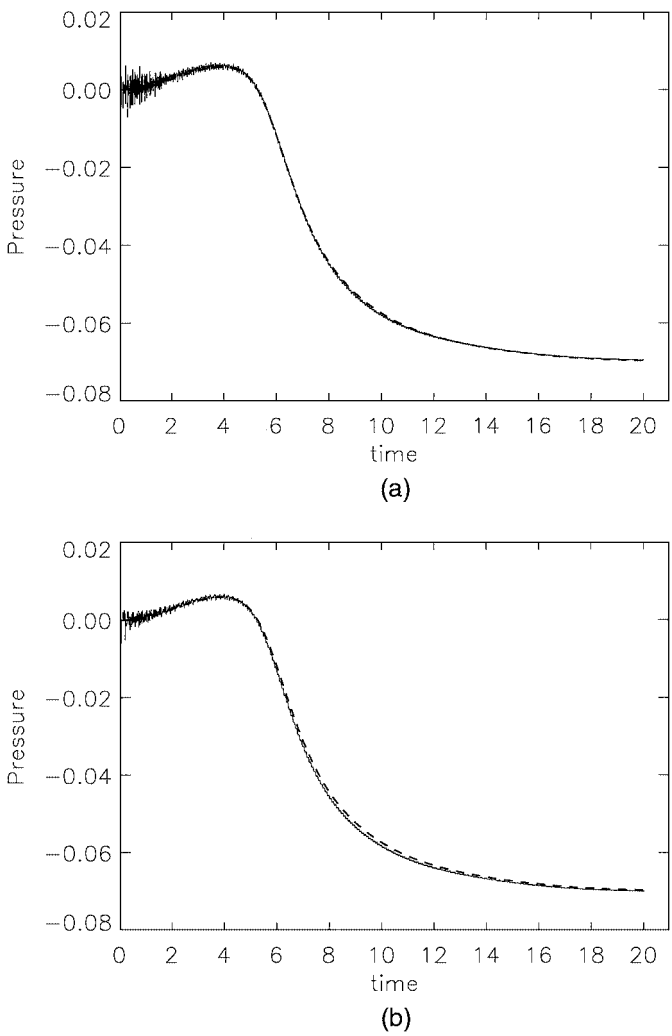

FIG. 5. Time history of pressure at the cavity center. The oscillations in pressure are much stronger than those in velocity for both (a) LBM and (b) AC methods. The dashed lines are results from the projection method.

the nondimensional characteristic time for the pressure wave propagations in the cavity ($2U/c_s$ or $2M$). The velocities from both the LBM and AC methods follow closely those obtained from the projection method.

The calculated pressures exhibit larger differences among the lattice Boltzmann, artificial compressibility, and projection methods (Fig. 4). These differences are most evident in the early stages ($t = 2.0$ and 4.0), where a horizontal pressure gradient exists cross the cavity in the background for both LBM and AC results. This pressure gradient is associated with the pressure wave bouncing back and forth between the left and right walls. The pressure gradient gradually dissipates and is invisible at $t = 14$.

The pressure wave can be better revealed from the time history of pressure at the middle of the cavity (Fig. 5). Obviously, the pressure oscillation is much stronger than the velocity oscillation, especially in early stages ($t < 4.0$). Nevertheless, the overall results from both LBM and AC are consistent with those obtained from the projection method.

It is interesting to note that, contrary to the velocity results, the pressure results from LBM and AC simulations differ significantly from each other at early times (Fig. 6). Although the AC simulation did not capture the sharp corners in the velocity history, as the LBM

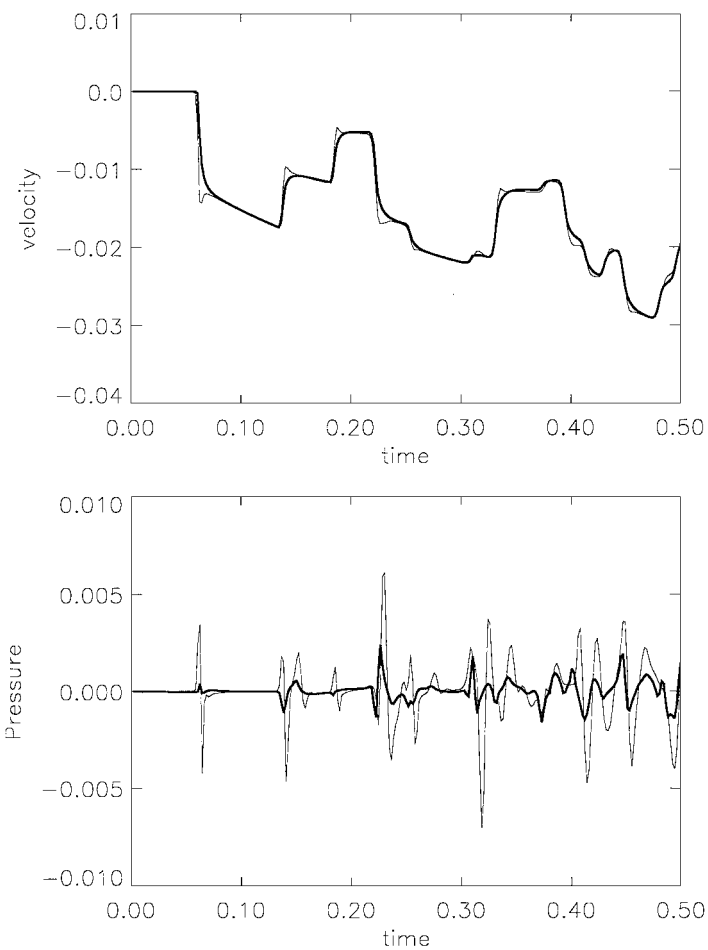

FIG. 6. Comparison of early stage velocity and pressure for LBM (thin lines) and AC methods (thick lines). The agreement is much better for the velocity results than for the pressure results.

simulation did, the velocity results at least follow with each other. The pressure histories, however, differ considerably from each other at early times. There are indications [20] that the LBM captures pressure waves accurately and this may be an area where LBM works better than the artificial compressibility method.

Several sources could contribute to the pressure field discrepancy between LBM and AC methods. In addition to the difference in stencil selection and temporal discretization, the lattice Boltzmann method also differs from the artificial compressibility method in its boundary conditions. Which factor plays the more important role warrants more study.

V. CONCLUSION

In conclusion, we have compared in detail the lattice Boltzmann method and the artificial compressibility method. It was found that these two methods are closely related to each other. Both of them satisfy similar macroscopic equations and their computational speeds are comparable. Although these two methods differ in discrete forms, they yield almost the same results for velocity fields. In simulations of transient flow, both methods exhibit oscillatory features but otherwise follow the incompressible flow very well. These results indicate that both the lattice Boltzmann method and artificial compressibility method can be used to study transient fluid flows. The pressure wave is a real physical phenomenon for compressible flows. The amplitude of the accoustic waves can be reduced if proper parameters are used.

The major difference between the LBM and AC simulations resides in the pressure results. The simulated pressure fields exhibited a significant difference. Considering the fact that the lattice Boltzmann method starts with the kinetic theory and has been derived to conserve high-order isotropy, the lattice Boltzmann method should be more accurate than the artificial compressibility method in capturing pressure waves. If used to simulate single-phase weakly compressible flows and if pressure waves are of interest, the lattice Boltzmann method may have a clear advantage over the artificial compressibility method in this limit.

APPENDIX

With the equilibrium distribution Eq. (2) and the lattice velocity satisfying Eqs. (5) and (6), we can obtain the following moments of the equilibrium distribution:

$$\sum f_\alpha^{eq} = pM^2,$$
$$\sum f_\alpha^{eq}\mathbf{e}_a = \mathbf{u}M,$$
$$\sum f_\alpha^{eq}\mathbf{e}_a^2 = (p\boldsymbol{\delta} + \mathbf{uu})M^2,$$
$$\sum f_\alpha^{eq}\mathbf{e}_a^3 = \delta^2 \cdot \mathbf{u}M.$$

Using the first-order Chapman–Enskog expansion, we can express the nonequilibrium distribution as

$$f_\alpha^1 = -\tau\left(\partial_{t_0} + M^{-1}\mathbf{e}_a \cdot \nabla\right) f_\alpha^{eq}. \tag{28}$$

The moments of the nonequilibrium distribution can be calculated accordingly:

$$\sum f_\alpha^1 = 0,$$
$$\sum f_\alpha^1 \mathbf{e}_a = 0,$$
$$\sum f_\alpha^1 \mathbf{e}_a^2 = -\tau[\nabla \mathbf{u} + (\nabla \mathbf{u})^T].$$

ACKNOWLEDGMENT

This research is supported by the Department of Energy under Contract W-7405-ENG-36.

REFERENCES

1. S. Chen and G. D. Doolen, Lattice Boltzmann method for fluid flows, *Annu. Rev. Fluid Mech.* **30**, 329 (1998).
2. G. R. McNamara and G. Zanetti, Use of the Boltzmann equation to simulate lattice-gas automata, *Phys. Rev. Lett.* **61**, 2332 (1998).
3. U. Frisch, D. d'Humières, B. Hasslacher, *et al.*, Lattice gas hydrodynamics in two and three dimensions, *Complex Syst.* **1**, 649 (1987).
4. X. Y. He and L. S. Luo, Lattice Boltzmann model for the incompressible Navier–Stokes equation, *J. Stat. Phys.* **88**, 927 (1997).
5. S. Chapman and T. G. Cowling, *The Mathematical Theory of Non-Uniform Gases* (Cambridge Mathematical Library, Cambridge, UK 1970), 3rd ed.
6. D. O. Martinez, W. H. Matthaeus, S. Chen, *et al.*, Comparison of spectral method and lattice Boltzmann simulations of 2-dimensional hydrodynamics, *Phys. Fluids* **6**, 1285 (1994).
7. S. L. Hou, Q. S. Zou, S. Y. Chen, G. Doolen, and A. C. Cogley, Simulation of cavity flow by the lattice Boltzmann method, *J. Comput. Phys.* **118**, 329 (1995).
8. X. Y. He and G. Doolen, Lattice Boltzmann method on curvilinear coordinates system: Flow around a circular cylinder, *J. Comput. Phys.* **134**, 306 (1997).
9. A. J. Chorin, A numerical method for solving incompressible viscous flow problems, *J. Comput. Phys.* **2**, 12 (1967).
10. X. Y. He and L. S. Luo, *A priori* derivation of the lattice Boltzmann equation, *Phys. Rev. E* **55**, R6333 (1997).
11. W. R. Osborn, E. Orlandini, M. R. Swift, *et al.*, Lattice Boltzmann study of hydrodynamic spinodal decomposition, *Phys. Rev. Lett.* **75**, 4031 (1995).
12. H. D. Chen, B. M. Boghosian, P. V. Coveney, and M. Nekovee, A ternary lattice Boltzmann model for amphiphilic fluids, *Proc. R. Soc. London Ser. A* **456**, 2043 (2000).
13. X. Y. He, R. Y. Zhang, S. Y. Chen, and G. D. Doolen, On the three-dimensional Rayleigh–Taylor instability," *Phys. Fluids* **11**, 1143 (1999).
14. X. Y. He and L. S. Luo, Theory of the lattice Boltzmann method: From the Boltzmann equation to the lattice Boltzmann equation, *Phys. Rev. E* **56**, 6811 (1997).
15. H. Grad, Note on N-dimensional Hermite polynomials," *Commun. Pure Appl. Math.* **2**, 325 (1949).
16. H. Grad, On the kinetic theory of rarefied gases, *Commun. Pure Appl. Math.* **2**, 331 (1949).
17. R. Peyret and T. D. Taylor, *Computational Methods for Fluid Flow* (Springer-Verlag, Berlin/New York, 1983).
18. F. H. Harlow and J. E. Welch, Numerical calculation of time-dependent viscous incompressible flow of fluid with free surface, *Phys. Fluids* **8**, 2182 (1965).
19. U. Ghia, K. N. Ghia, and C. T. Shin, High-Re solutions for incompressible-flow using Navier–Stokes equations and a multigrid method, *J. Comput. Phys.* **48**, 387 (1982).
20. L.-J. Huang, private communication.